Heterogeneous Catalysis

DOI: 10.1002/anie.200703481

Aqueous-Phase Fischer–Tropsch Synthesis with a Ruthenium Nanocluster Catalyst**

Chao-xian Xiao, Zhi-peng Cai, Tao Wang, Yuan Kou, and Ning Yan**

Hydrogenation of carbon monoxide to produce hydrocarbons, normally called Fischer–Tropsch synthesis (F–T synthesis),[1] is one of the most important hydrogenation reactions owing to its potential for the intermediate production of hydrocarbon fuels in the "postpetroleum" era. Supported and unsupported catalysts have been widely investigated over the last 80 years or more,[2] and it is unlikely that further major improvements in the economic and energy efficiencies of the process can be realized with conventional catalysts. The reaction is favored at low temperature; therefore, reducing the particle size of the catalyst to several nanometers, while maintaining the three-dimensional freedom of the particles, may in principle significantly increase the catalytic activity as well as decrease the working temperatures for the process. It has been reported that soluble nanoclusters[3] in ionic liquids[4] or liquid water[5] exhibit excellent catalytic performance in the hydrogenation of various organic substrates and also are comparatively green in nature.[6] As far as we are aware, aqueous-phase F–T synthesis has not been reported to date, but it has been shown[7] that water promotes the reaction—for example, the activity (calculated on the basis of the total number of Ru atoms) of a traditional 5% Ru/SiO_2 catalyst was increased by a factor of 3 when the pressure of steam was increased from 0.017 to 0.454 MPa (see entry 15 in Table 1).[7a] Herein we report our first steps in the development of an aqueous-phase process for the hydrogenation of carbon monoxide using a ruthenium nanocluster catalyst.

Water-soluble ruthenium(0) nanoclusters with a diameter of 2.0 ± 0.2 nm (see Figure 2a) were prepared by the reduction of ruthenium trichloride hydrate under 2.0 MPa H_2 in the presence of poly(*N*-vinyl-2-pyrrolidone) (PVP). The results shown in Table 1 were obtained by sealing the syngas (3.0 MPa, $H_2/CO = 2{:}1$) in a stainless steel autoclave running in batch mode. A high-precision pressure gauge was used to monitor the reaction and to calculate the catalytic activity. It can be seen that a nanocluster ruthenium catalyst stabilized by an ionic-liquid-like copolymer[6a,b] in the ionic liquid $[BMIM][BF_4]$ (Table 1, entry 11) afforded an acceptable activity of 0.55 $mol_{CO}\,mol_{Ru}^{-1}\,h^{-1}$ for the synthesis at 150 °C and total pressure of 3.0 MPa. Similar activities were obtained when using ethanol, dioxane, or cyclohexane as solvent (Table 1, entries 7, 9, and 10, respectively). Addition of water to the ethanol system gave a significant enhancement in activity (Table 1, entry 8). This result prompted us to conduct the synthesis in pure liquid water under the same conditions, which led to an unprecedented activity of as high as 6.9 $mol_{CO}\,mol_{Ru}^{-1}\,h^{-1}$ (Table 1, entries 2,3). This value is almost 35 times that of the above-mentioned Ru/SiO_2 catalyst at 150 °C (Table 1, entry 14) and 6–16 times that of the same catalyst at 200 °C (Table 1, entry 15) in the presence of varied amounts of added steam (see also Table S1 in the Supporting Information for more information about traditional cata-

Table 1: Catalytic properties of Ru nanoclusters in various solvents[a] and comparative data for conventional supported catalysts.

Entry	Solvent	Reducing agent[b]	*T* [°C]	Activity [$mol_{CO}\,mol_{Ru}^{-1}\,h^{-1}$]	Aggregation after reaction
1	water	blank	150	0	–
2[c]	water	H_2	150	6.8	no
3	water	H_2	150	6.9	no
4	water	H_2	120	3.1	no
5	water	H_2	100	0.74	no
6	water	$NaBH_4$	150	1.6	no
7	ethanol	H_2	150	0.32	no
8[d]	ethanol	H_2	150	0.78	no
9	dioxane	H_2	150	0.42	no
10	cyclohexane	H_2	150	0.65	yes
11[e]	$[BMIM][BF_4]$	H_2	150	0.55	no
12[e]	$[BMIM][BF_4]$	$NaBH_4$	150	0.18	no
13	5% Ru/C in 20 mL water		150	0	–
14[f]	8% Ru/SiO_2, 0.1 MPa, $H_2/CO = 1$, 500 mL h^{-1}		150	0.19	–
15[g]	5% Ru/SiO_2, 1.5 MPa, $H_2/CO = 2$, $p(H_2O) = 0.017$–0.454 MPa		200	0.41–1.22	–

[a] Typical reaction conditions: 2.0 MPa H_2, 1.0 MPa CO, 20 mL solvent, 2.79×10^{-4} mol Ru, PVP/Ru = 20:1. [b] Used for preparing the ruthenium nanocluster catalysts. [c] PVP/Ru = 40:1. [d] Addition of 10.0 mL water. [e] An ionic-liquid-like copolymer poly[(*N*-vinyl-2-pyrrolidone)-*co*-(1-vinyl-3-alkylimidazolium halide)] was used to replace PVP, with copolymer/Ru = 5:1. BMIM = 1-*n*-butyl-3-methylimidazolium. [f] From literature data.[8] [g] From literature data.[7a]

[*] Dr. C.-X. Xiao, Z.-P. Cai, T. Wang, Prof. Dr. Y. Kou, N. Yan
PKU Green Chemistry Center
Beijing National Laboratory for Molecular Sciences
College of Chemistry and Molecular Engineering
Peking University
Beijing 100871 (China)
Fax: (+86) 10-6275-1708
E-mail: yuankou@pku.edu.cn
ynyy@pku.edu.cn

[**] This work was supported by the National Science Foundation of China (Projects 20533010, 20473002, and 20333020). The authors thank Drs. Jiangang Chen, Yuhan Sun, and Haichao Liu for useful discussions.

Supporting information for this article, including detailed experimental procedures, is available on the WWW under http://www.angewandte.org or from the author.

lysts). Indeed, even at 100 °C (Table 1, entry 5) the activity of the ruthenium nanocluster catalyst in water is comparable to that of the supported Ru/SiO_2 catalyst at 200 °C (Table 1, entry 15). The method of preparation of the ruthenium nanoclusters also affects the catalytic activity—for example, when $NaBH_4$ was used as the reducing agent, the activity of the resulting nanoclusters was only 1/3–1/4 of that of those prepared using H_2 as the reducing agent (Table 1, entries 6 and 12). It is noteworthy that a commercial Ru/C catalyst showed no detectable activity at 150 °C under identical reaction conditions to those employed for the nanoclusters (Table 1, entry 13).

The products of the F–T synthesis were carefully analyzed by well-established methods (see the Supporting Information), and the product distributions are shown in Figure 1 a. It is notable that C_5–C_{20} hydrocarbons made up the

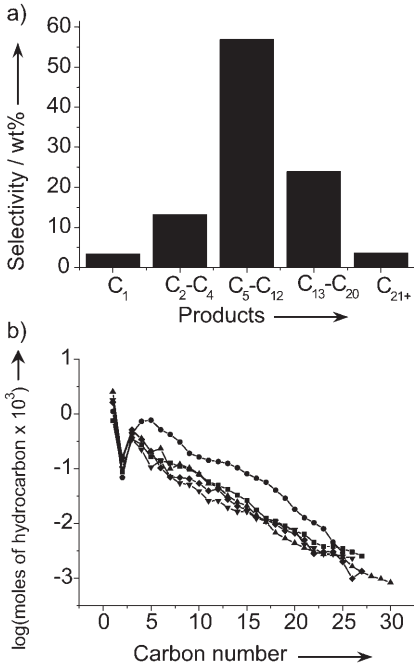

Figure 1. a) Hydrocarbon selectivities for 2.0-nm-diameter nanoclusters; b) Anderson–Schulz–Flory distribution of products for Ru nanocluster catalysts with different diameters of 1.8 ± 0.3 nm (■), 2.0 ± 0.2 nm(●), 2.5 ± 0.3 nm (▲), 2.9 ± 0.3 nm (▼), 3.3 ± 0.4 nm (◆). Reaction conditions: 150 °C, 2.0 MPa H_2, 1.0 MPa CO, 2.79×10^{-4} mol Ru, 20 mL water, PVP/Ru = 40:1 (PVP/Ru = 200:1 for 1.8-nm-diameter nanoclusters).

vast majority (80.9 wt %) of the products, and that only 3.3 wt % of methane was formed. No oxygenates were detected in either the organic phase or the aqueous phase. The linear trend in Figure 1 b clearly demonstrates that the chain length distribution of the reaction products follows the Anderson–Schulz–Flory statistics.

The transmission electron microscopy (TEM) characterization (Figure 2) showed that the particle size of freshly prepared ruthenium nanoclusters had a very narrow distribution. The TEM micrograph of the 2.0-nm nanoclusters is shown in Figure 2 a and indicates that that the deviation from

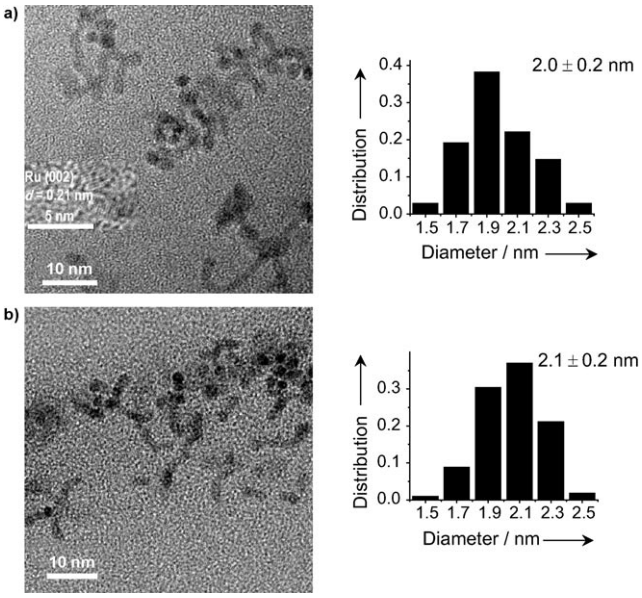

Figure 2. TEM micrographs and size distributions of Ru nanoclusters: a) freshly prepared, inset: high-resolution TEM image; b) after reaction. Reaction conditions: 150 °C, 2.0 MPa H_2, 1.0 MPa CO, 2.79×10^{-4} mol Ru, 20 mL water, PVP/Ru = 40:1.

the mean diameter is about ± 0.2 nm. The average particle size increased slightly to 2.1 nm with the same deviation of 0.2 nm after reaction (Figure 2 b), indicating that the ruthenium nanoclusters appear to be stable under the reaction conditions.

To examine the stability of the 2.0-nm nanocluster catalyst in more detail, the reaction was carried out in a semibatch mode for 48 h, that is, whenever the pressure dropped below 1.2 MPa, additional syngas was supplied to the reactor to restore the pressure to the initial value of 3.0 MPa. The activity dropped from 6.9 $mol_{CO}\,mol_{Ru}^{-1}\,h^{-1}$ at the beginning of the reaction to about 4.0 $mol_{CO}\,mol_{Ru}^{-1}\,h^{-1}$ after 8 h, and then remained at this value over the next 40 h, thus demonstrating the long-term stability of the catalyst. After the reaction was quenched, liquid hydrocarbons and solid wax were present as the top layer in the reactor, well separated from the bottom aqueous layer, indicating the ease of separation for products and catalyst in this reaction system (Figure S1 in the Supporting Information). No precipitate was observed in the bottom aqueous layer. Analysis by inductively coupled plasma (ICP) emission spectroscopy of the hydrocarbon layer showed no leaching of Ru within the detection limit (ca. 0.05 $\mu g\,L^{-1}$).

Detailed studies show that the diameter of the Ru nanoclusters did not have a significant effect on the chain length distribution of the F–T products (Figure 1 b, and Figure S2 in the Supporting Information). However, it had a significant effect on the catalytic activity. As shown in Figure 3 a, the catalytic activity showed a slight increase when the particle diameter was reduced from 4.0 to 2.5 nm, but a dramatic increase when the diameter was reduced to 2.0 nm. Further reducing of the particle diameter to 1.8 nm, however, resulted in a sharp fall in activity (this result cannot be explained by the inhibiting effect of the additional

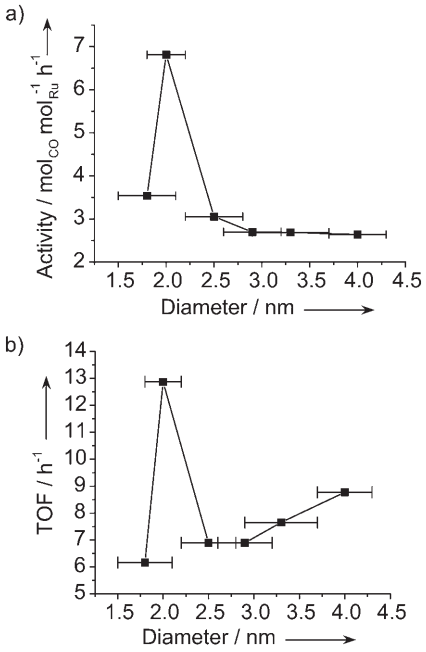

Figure 3. a) Catalytic activity and b) TOF as a function of diameter of the Ru nanoclusters. Reaction conditions: 150 °C, 2.0 MPa H_2, 1.0 MPa CO, 2.79×10^{-4} mol Ru, 20 mL water, PVP/Ru = 40:1 (PVP/Ru = 200:1 for 1.8-nm nanoclusters).

stabilizer required to prepare the 1.8-nm nanoclusters; see the Supporting Information for details). The surface-specific activity, referred to as turnover frequency (TOF, the activity calculated on the basis of the number of surface atoms; see the Supporting Information for details) decreased gradually as the size of the nanoclusters was reduced from 4.0 to 2.5 nm (Figure 3b) and then increased dramatically to an unprecedented maximum value of 12.9 h^{-1} for the nanoclusters with a diameter of 2.0 nm, before decreasing significantly again for the 1.8-nm-diameter nanoclusters. Despite efforts to rationalize this very unusual phenomenon, no atomic-level explanation is currently available.

The aqueous-phase F–T synthesis demonstrated here offers opportunities to reexamine this long-established process from various aspects. Firstly, in the case of conventional supported ruthenium F–T catalysts, the support effects have been widely studied.[9] The catalytic activities were found to be influenced largely by the different supports employed and were attributed to electronic, geometric, or other effects (e.g. surface lattice vacancies). Our work, however, shows that ruthenium nanoclusters themselves in the absence of any support show much higher catalytic activity than that of supported catalysts. This finding reflects that the intrinsic effects of supports may need to be reconsidered.

Secondly, commercial F–T synthesis processes usually use slurry reactors with CO and H_2 circulating through wax. Our aqueous-phase F–T synthesis offers the opportunity to employ a reactor with all the advantages of the traditional slurry reactor coupled with facile product separation resulting from the immiscibility of the hydrocarbon products and the water-soluble catalyst.

Finally, the mechanism of F–T synthesis is very complicated and has not been fully delineated. The ruthenium nanoclusters in our system are homogenously dispersed in a solvent, which allows us to study the mechanism of the process by using the array of spectroscopic techniques which have been proven to be very successful in exploring homogeneous catalysts. In fact, in situ infrared and Raman spectroscopic investigations are currently underway in our laboratory.

In conclusion, aqueous-phase F–T synthesis with a TOF of 12.9 h^{-1} has been realized over a ruthenium nanocluster catalyst (with a mean diameter of 2.0 nm) at 150 °C under 2.0 MPa H_2 and 1.0 MPa CO. This is the first example demonstrating that a very important industrial process generally carried out using supported metal catalysts can be realized by soluble metal nanocluster catalysts, with much enhanced catalytic efficiencies.

Experimental Section

The aqueous-phase ruthenium nanocluster catalyst was prepared according to the following procedure: $RuCl_3{\cdot}nH_2O$ (73 mg, 2.79×10^{-4} mol Ru) and PVP (1.240 g, 1.12×10^{-2} mol; PVP/Ru = 40:1) were dissolved in deionized water (20 mL) with stirring. The solution was placed in a 60-mL stainless steel autoclave equipped with a high-precision pressure gauge (±0.4%). The catalyst was reduced under 2.0 MPa H_2 at 150 °C for 2 h with a stirring speed of 800 rpm. The resulting colloidal black solution contained ruthenium nanoclusters with an average diameter of 2.0 ± 0.2 nm. Ruthenium nanoclusters with diameter 1.8 ± 0.3 nm were prepared under the same conditions with the addition of a larger amount of PVP (PVP/Ru = 200:1). A series of larger ruthenium nanoclusters (diameter 2.5–4.0 nm) were prepared by reduction of $RuCl_3{\cdot}nH_2O$ by 2.0 MPa H_2 at 60 °C in the presence of the smaller ruthenium nanoclusters.

For catalytic testing, a solution of the freshly prepared Ru nanoclusters (2.79×10^{-4} mol Ru) was placed in a 60-mL stainless steel autoclave and heated in the presence of 1.0 MPa CO (99.9%, purified by activated 5-Å molecular sieves) and 2.0 MPa H_2 (99.999%). The autoclave was kept at 150 °C with stirring at 800 rpm until the total pressure decreased to about 1.2 MPa (or about 0.75 MPa at room temperature, corresponding to a CO conversion of about 75%). After reaction, the autoclave was cooled to room temperature. The products were collected and analyzed by GC, GC–MS, and IR.

Received: August 1, 2007
Revised: November 5, 2007
Published online: December 7, 2007

Keywords: heterogeneous catalysis · hydrogenation · nanostructures · ruthenium

[1] a) F. Fischer, H. Tropsch, *Brennst.-Chem.* **1923**, *4*, 276–285; b) F. Fischer, H. Tropsch, *Brennst.-Chem.* **1926**, *7*, 97–104.
[2] a) R. B. Anderson, *The Fischer–Tropsch Synthesis*, Academic Press, London, **1984**, pp. 100–173; b) M. Röper in *Catalysis in C1 Chemistry* (Ed.: W. Keim), D. Reidel, Dordrecht, **1983**, pp. 41–88; c) A. A. Adesina, *Appl. Catal. A* **1996**, *138*, 345–367; d) Y. T. Shah, A. J. Perrotta, *Ind. Eng. Chem. Prod. Res. Dev.* **1976**, *15*, 123–131.
[3] a) T. Welton, *Chem. Rev.* **1999**, *99*, 2071–2083; b) P. Wasserscheid, W. Keim, *Angew. Chem.* **2000**, *112*, 3926–3945; *Angew. Chem. Int. Ed.* **2000**, *39*, 3772–3789; c) D.-B. Zhao, M. Wu, Y.

Kou, E. Min, *Catal. Today* **2002**, *74*, 157 – 189; d) J. Dupont, R. F. de Souza, P. A. Z. Suarez, *Chem. Rev.* **2002**, *102*, 3667 – 3691.

[4] a) J. S. Bradley, G. Schmid in *Nanoparticles: From Theory to Application* (Ed.: G. Schmid), Wiley-VCH, Weinheim, **2004**, pp. 185 – 199; b) D. Astruc, F. Lu, J. R. Aranzaes, *Angew. Chem.* **2005**, *117*, 8062 – 8083; *Angew. Chem. Int. Ed.* **2005**, *44*, 7852 – 7872; c) H. Bönnemann, R. M. Richards, *Eur. J. Inorg. Chem.* **2001**, 2455 – 2480; d) J. D. Aiken III, R. G. Finke, *J. Mol. Catal. A* **1999**, *145*, 1 – 44; e) A. Roucoux, J. Schulz, H. Patin, *Chem. Rev.* **2002**, *102*, 3757 – 3778.

[5] a) J. Schulz, A. Roucoux, H. Patin, *Chem. Eur. J.* **2000**, *6*, 618 – 624; b) M. Zhao, R. M. Crooks, *Angew. Chem.* **1999**, *111*, 375 – 377; *Angew. Chem. Int. Ed.* **1999**, *38*, 364 – 366.

[6] a) X.-D. Mu, J.-Q. Meng, Z.-C. Li, Y. Kou, *J. Am. Chem. Soc.* **2005**, *127*, 9694 – 9695; b) C. Zhao, H.-Z. Wang, N. Yan, C.-X. Xiao, X.-D. Mu, P. J. Dyson, Y. Kou, *J. Catal.* **2007**, *250*, 33 – 40; c) C.-X. Xiao, H.-Z. Wang, X.-D. Mu, Y. Kou, *J. Catal.* **2007**, *250*, 25 – 32; d) N. Yan, C. Zhao, C. Luo, P. J. Dyson, H. Liu, Y. Kou, *J. Am. Chem. Soc.* **2006**, *128*, 8714 – 8715.

[7] a) M. Claeys, E. van Steen, *Catal. Today* **2002**, *71*, 419 – 427; b) C. J. Kim, US Patent 0355218, **1993**; c) C. J. Kim, US Patent 5227407, **1993**.

[8] M. L. Turner, N. Marsih, B. E. Mann, R. Quyoum, H. C. Long, P. M. Maitlis, *J. Am. Chem. Soc.* **2002**, *124*, 10456 – 10472.

[9] a) E. Kikuchi, H. Nomura, M. Matsumoto, Y. Morita, *Appl. Catal.* **1983**, *7*, 1 – 9; b) D. L. King, *J. Catal.* **1978**, *51*, 386 – 397; c) E. Iglesia, S. L. Soled, R. A. Fiato, *J. Catal.* **1992**, *137*, 212 – 224; d) T. Komaya, A. T. Bell, W. Zara, R. Gronsky, F. Engleke, T. S. King, M. Pruski, *J. Catal.* **1994**, *150*, 400 – 406.

